Journal of Power Sources 196 (2011) 2635–2639

Contents lists available at ScienceDirect

Journal of Power Sources

journal homepage: www.elsevier.com/locate/jpowsour

Short communication

Simultaneous visualization of oxygen distribution and water blockages in an operating triple-serpentine polymer electrolyte fuel cell

Kenji Takada[a], Yuta Ishigami[a], Junji Inukai[a,*], Yuzo Nagumo[b], Hiroshi Takano[c], Hiroyuki Nishide[d,**], Masahiro Watanabe[a,***]

[a] University of Yamanashi, 4 Takeda, Kofu, Yamanashi 400-8510, Japan
[b] Shimadzu, 3-9-4 Hikaridai, Seika-Cho, Kyoto 619-0237, Japan
[c] Fuji Electric Holdings, 7 Yawata-Kaigandori, Ichihara, Chiba 290-8511, Japan
[d] Waseda University, 3-4-1 Okubo, Shinjuku, Tokyo 169-8555, Japan

ARTICLE INFO

Article history:
Received 30 July 2010
Received in revised form 23 October 2010
Accepted 28 October 2010
Available online 3 November 2010

Keywords:
Fuel Cell
Simultaneous visualization
Porphyrin
Oxygen partial pressure
Flooding
Gas diffusion layer

ABSTRACT

Visualization inside polymer electrolyte fuel cells (PEFCs) is important for elucidating reaction distributions to improve the performance and durability of the cells. An O_2-sensitive porphyrin luminescent dye film was used to visualize oxygen partial pressures and water blockages simultaneously in triple-serpentine gas flow channels in an operating PEFC. Water droplets formed near the exit of a gas-flow channel lowered the oxygen partial pressure noticeably over the channel by blocking air flow near the entrance. Meanwhile, air was continuously supplied from the other channels through the gas diffusion layer, thus allowing power to be generated in the blocked channel. With water blockages, however, the catalyst layer under the channel became flooded by the water produced during the reaction, and the flooded state continued to exist in the catalyst and/or porous layers, even after blowing the water droplet out, so that the power generation was lowered along the channel.

1. Introduction

Polymer electrolyte fuel cells (PEFCs) produce electricity directly from hydrogen and oxygen and are expected to be used in automobiles, residences, and portable devices, generating very low levels of emissions. To enhance the possibilities for commercialization, higher performance, lower cost, and higher durability are still required. In PEFCs, insufficiencies in the proton network and membrane degradation can occur as a result of membrane drying out [1–3]. Excess water, on the other hand, blocks gas flow channels and hinders gas access to active catalyst areas, resulting in significant performance drops [4,5]. Water management is, therefore, one of the most important issues in PEFCs [6]. Thus far, liquid water distribution in operating fuel cells has been visualized with a CCD camera [7–10] and by neutron scattering [11–14], NMR [15–17], and X-ray micro-morphological characterization techniques [18–20]. Computational calculations and simulations have aided the understanding of these experimental results [21]. Although the distributions of liquid water in PEFCs have been widely studied by the visualization techniques stated above, there has been little research on how liquid water droplets affect the reaction distributions in PEFCs.

In earlier studies, we have succeeded in visualizing the oxygen partial pressures in an operating PEFC with various oxygen partial pressures [22] and a direct methanol fuel cell (DMFC) with changing current densities [23] by using an O_2-sensitive porphyrin luminescent dye film. Water droplets were also visualized with this visualization technique [23]. In this paper, we succeeded in visualizing oxygen partial pressures and water blockages simultaneously in an operating PEFC. The relationship between water blockages in flow channels and oxygen partial pressures in an operating PEFC is discussed.

2. Experimental

Instrumental setups for visualization are reported in detail elsewhere [22,23]. In this study, a PEFC with triple-serpentine flow channels (1065 mm long for each channel) was used (Fig. 1). Briefly, a dye film (tetrakis(pentafluorophenyl) porphyrinatoplatinum + poly(1-trimethylsilyl-1-propyne)) was coated on the upper part of the cathode flow channels of a sep-

* Corresponding author at: University of Yamanashi, Fuel Cell Nanomaterials Center, 6-43 Miyamae-Cho, Kofu, Yamanashi 400-002, Japan. Tel.: +81 55 254 7129; fax: +81 55 254 7129.
** Corresponding author. Tel.: +81 3 3200 2669; fax: +81 3 3209 5522.
*** Corresponding author. Tel.: +81 55 254 7091; fax: +81 55 254 7091.
E-mail address: jinukai@yamanashi.ac.jp (J. Inukai).

0378-7753/$ – see front matter © 2010 Elsevier B.V. All rights reserved.
doi:10.1016/j.jpowsour.2010.10.097

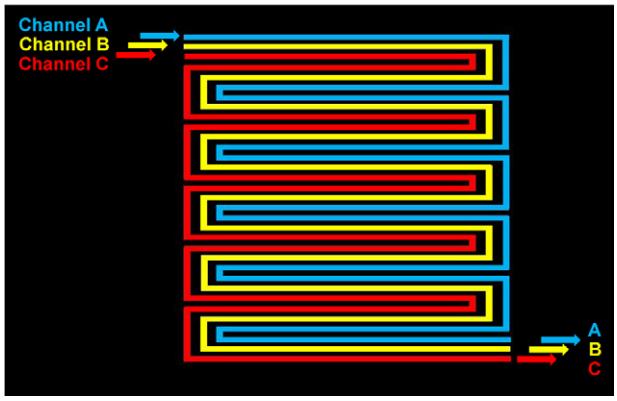

Fig. 1. Schematic drawing of the triple-serpentine gas-flow channels (Channels A–C) at the cathode of the visualization cell. Channel length = 1065 mm; rib width = 1 mm; channel width = 2 mm; channel depth = 1 mm.

arator, made of transparent polyacryl resin, as an oxygen sensor. Laser light (407 nm) was irradiated, the emission from the cell was filtered (>610 nm), and images were captured with a CCD camera. Calibration curves were obtained before the cell operation with variation of the oxygen partial pressure inside the cell. By use of the calibration curves, the emission signals from the cell were converted to oxygen partial pressures with a space resolution of 0.2 mm and a time resolution of 0.5 s. Water droplets were also observed with this instrumental setup [23]. During the cell operation, the cell was operated at 70 °C and 90% RH, with a gas flow rate of 100 mL min^{-1}. Oxygen utilization was 80% at a current density of 48 mA cm^{-2}. At higher current densities with higher gas flow rates, the water droplets were removed, and no water blockages were formed.

3. Results and discussion

3.1. Simultaneous visualization of water blockage and oxygen partial pressure

Fig. 2(a) shows the oxygen partial pressure inside a triple-serpentine PEFC. Three gas-flow channels, Channels A–C (see Fig. 1), are indicated by arrows. Fig. 2(a) was taken 2 min after cell startup at a current density of 48 mA cm^{-2}; cell temperature = 70 °C; relative humidity = 90% (air and H_2); each reactant gas flow = 100 mL min^{-1}, and the average utilization of oxygen in air = 90% at the channel exits. The oxygen partial pressure is seen to decrease gradually in similar manner for the three channels along the length. This gradual decrease has been also observed in a single-serpentine cell [22]. No water droplets are seen in the image. On the other hand, Fig. 2(b) is an image obtained 119 min after startup. The oxygen partial pressure is seen to be drastically decreased, nearly to 0 kPa, as indicated by the dark blue color in the latter part of Channel B. After obtaining Fig. 2(b), the cell operation was stopped. Fig. 2(c) shows an image after the cell operation was stopped, at the open circuit voltage (OCV) with no power generation. Interestingly, in Channel B, areas in blue are seen in some parts. These areas are associated with liquid water blockages in the gas flow channel, as reported previously [23]. These water blockages were also directly detected optically. In this way, both water blockages and oxygen partial pressures in the fuel cell were simultaneously visualized. The oxygen shortage in Channel B is now understood as being due to the formation of water blockages in the channel. The water blockages were formed and observed in all channels.

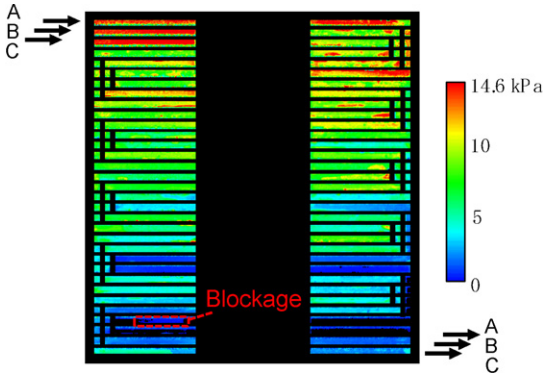

Fig. 3. Oxygen partial pressure visualized in an operating PEFC with a water blockage in Channel A.

3.2. Water blockages and oxygen shortages investigated by visualization

Fig. 3 shows an image of oxygen partial pressure with one area of water blockage in Channel A obtained after the cell had been operated with current flowing for some period of time, under the same conditions as those of Fig. 2. The blockage is indicated by a red rectangle around 960 mm from the entrance. Fig. 4 shows graphs for the oxygen partial pressures in Channels A–C along the channels, where the partial pressures were obtained from Figs. 2(a) and 3, respectively, for operation without water blockage (filled circles) and with blockage (open circles) in Channel A. In Channels B and C, oxygen partial pressures appeared to decrease monotonically along the channels, indicating the normal consumption of oxygen along the channel length, as shown in the previous work with the single-serpentine cell [22]. On the other hand, in Channel A, the

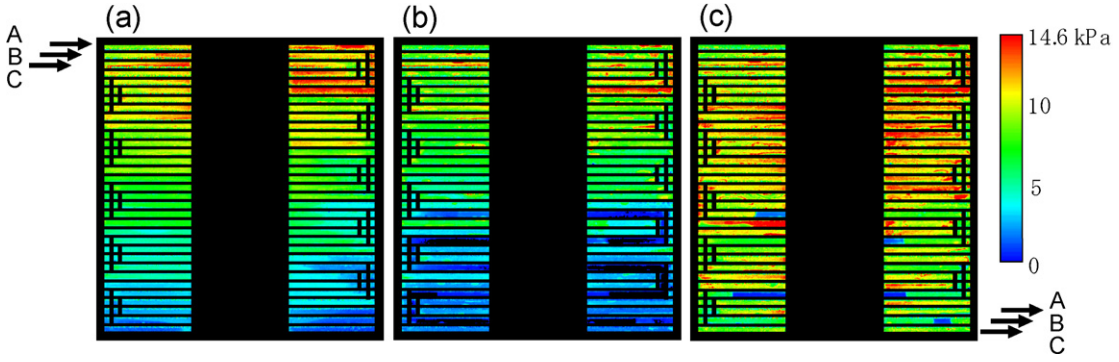

Fig. 2. Oxygen partial pressures visualized in an operating PEFC with/without water blockages in a flow channel: (a) without blockage, (b) with water blockages in Channel B, (c) with water blockages in Channel B after the operation was stopped, at the OCV. Cell temperature = 70 °C; relative humidity = 90% (air and H_2); gas flow = 100 mL min^{-1}, oxygen utilization = 80%, current density = 48 mA cm^{-2}.

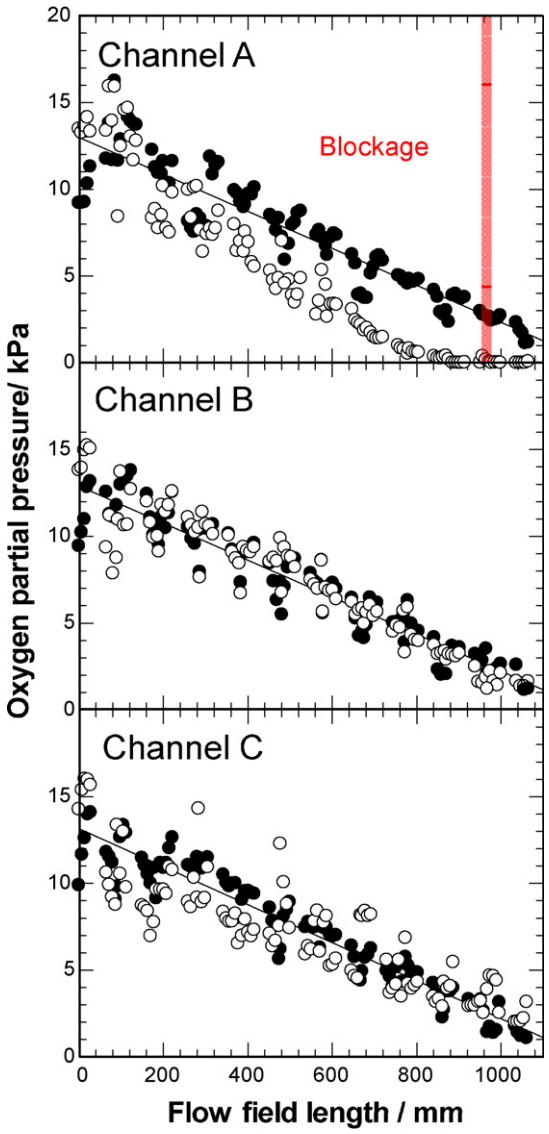

Fig. 4. Oxygen partial pressures without (●) and with (○) a water blockage in Channel A.

oxygen partial pressure was observed to be decreased to nearly 0 kPa around the water blockage (in the area from 800 mm to the exit). It is noteworthy that Channel A was completely blocked with the water droplet, but the oxygen partial pressure was maintained at a relatively high value along the channel, in spite of the continuous oxygen consumption, although it commenced to decrease more rapidly around 200 mm from the entrance toward the exit than is the case for normal consumption. This means that the air was not supplied to Channel A from the entrance but was transferred from the other channels through the gas diffusion layer (GDL). Therefore, in spite of the water blockage, power was still generated in Channel A. It might seem difficult for air to penetrate through the GDL from the other channels to the blocked channel. The GDL used was approximately 0.2-mm thick with a 75% space volume. Suppose the space volume becomes half under the ribs, the volume of the gas path under the GDL between two flow channels is equivalent to 8% of the volume of a flow channel. This volume should be large enough to allow the air diffusion between channels when air continuously flows in the non-blocked channels. It should also be noted that with one blocked channel, the velocity of air in the two non-blocked channels increases by approximately 50%. The higher gas velocity should increase the pressure in the non-blocked channels, too. Those effects apparently make the air penetration easier into the blocked channel.

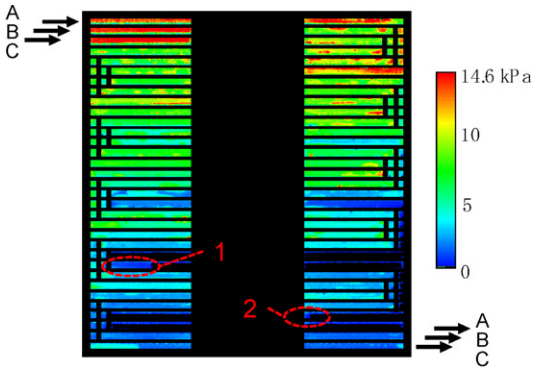

Fig. 5. Oxygen partial pressures visualized in an operating PEFC with two water blockages in Channel A.

In Channels B and C, although air was supplied to Channel A, the oxygen partial pressure did not show a large difference after the formation of a water blockage. When the gas flow from the entrance was blocked in Channel A, the total pressure, and hence the oxygen partial pressures, in Channels B and C must be increased, at least at the entrances. On the other hand, part of the air was transferred from Channels B and C to A, as discussed above. The power generation became lower in Channel A, so more electricity must have been produced, or more oxygen must have been consumed, in Channels B and C, in order to maintain the oxygen utilization of 80%, corresponding to the constant current flow. All of these situations being taken into account, the oxygen partial pressures in Channels B and C might have been practically the same, even after the formation of a water blockage in Channel A.

Fig. 5 shows the oxygen partial pressure with two water blockages, blockages 1 and 2, in Channel A, which are indicated by red circles. Fig. 6 shows the oxygen partial pressure changes in Channels A–C as a function of the flow field length. Oxygen partial pressures without water blockages (filled circles) and with blockages (open circles) in Channel A were obtained from Figs. 2(a) and 5, respectively. The positions of blockages 1 and 2 in Channel A are indicated by red marks. When water blockages were formed, the oxygen pressure became 0 kPa from 680 mm to the exit along Channel A. No increase in oxygen partial pressure was observed between blockages 1 and 2. The oxygen partial pressure started to decrease around 200 mm from the entrance, in a manner similar to that of one blockage (Fig. 4), but with two blockages, the oxygen partial pressures decreased more steeply. It is interesting to note that with two water blockages, the oxygen partial pressures in Channels B and C (open circles) are seen to become slightly lower than those with no water blockages (filled circles), which was not the case with one water blockage (Fig. 4). This might indicate that more oxygen is consumed in Channels B and C with two blockages than with one blockage in Channel A.

3.3. *Catalyst and/or gas-diffusion layers flooding with water blockage*

Fig. 7(a) shows an image for the oxygen partial pressure with one water blockage in Channel A. The oxygen pressure is approximately 0 kPa before and after the blockage, as also seen in Fig. 3. After obtaining Fig. 7(a), the water blockage was seen to be swept out to the exit. Fig. 7(b) is the image obtained immediately after the disappearance of the water blockage. Fig. 8 shows the oxygen partial pressures in the flow channels with the water blockage (open circles) and without the blockage (filled circles) in Channel A, which were obtained from Fig. 7(a) and (b), respectively. With the water

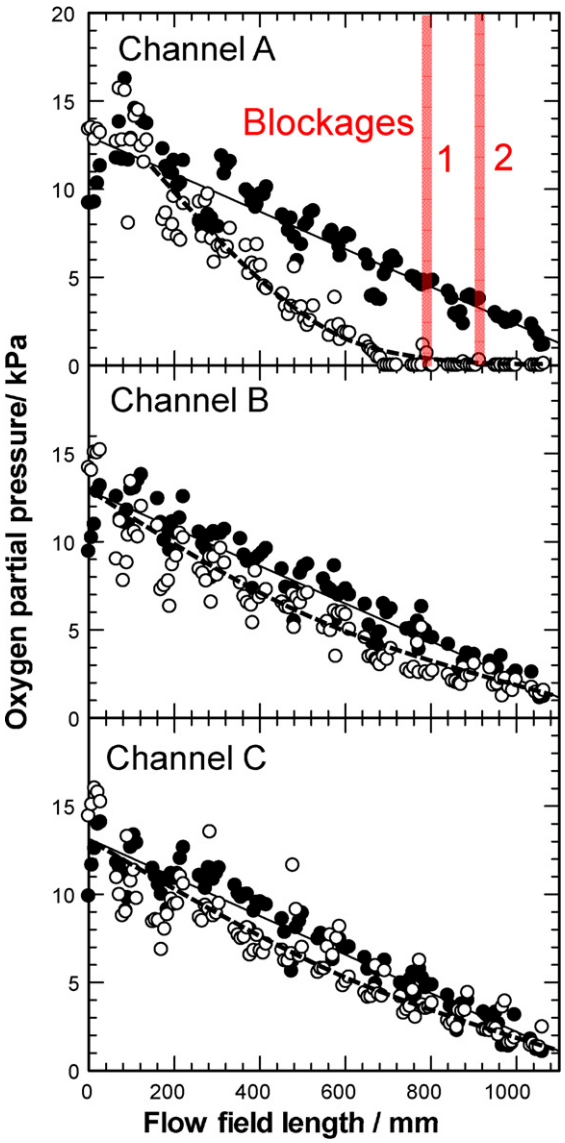

Fig. 6. Oxygen partial pressures without (●) and with (○) two water blockages in Channel A.

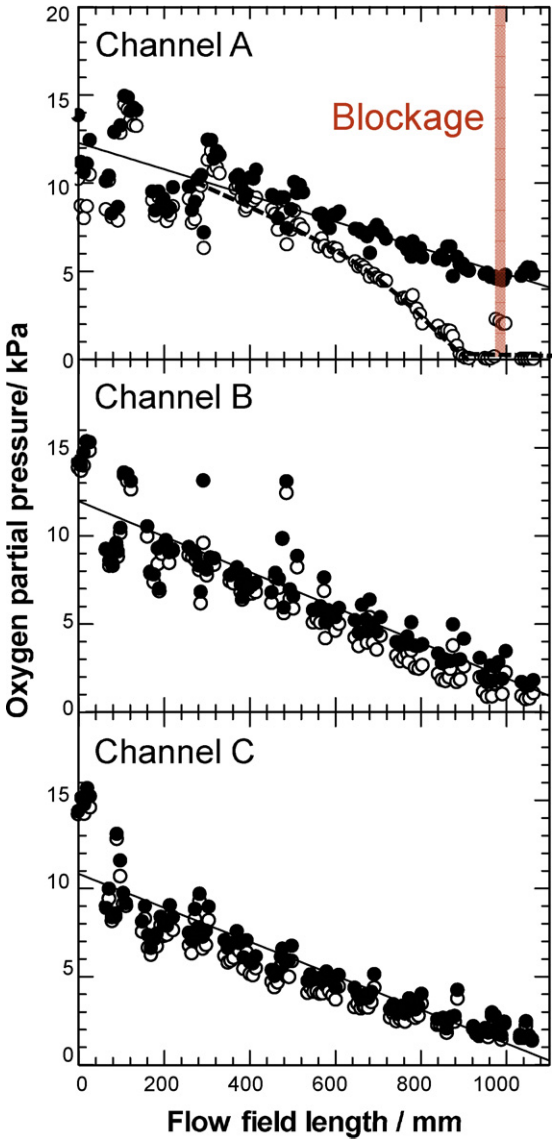

Fig. 8. Oxygen partial pressures in Channels A–C with a water blockage in Channel A (○) and after the removal of the water blockage (●).

blockage in Channel A, the distribution of oxygen partial pressure was nearly the same as that in Fig. 4. Notably, the oxygen partial pressure at the exit of Channel A increased to nearly 5 kPa after the removal of the water blockage. Oxygen partial pressures in Channels B and C did not show a large change. Since the oxygen partial pressure of Channel A became higher than that of normal operation (see Fig. 4(a)) or those of Channels B and C, the oxygen consumption along Channel A should be much smaller than those along Channels B and C. The lowered consumption may be explained as follows. As discussed in Fig. 4, air can be supplied from the other channels through the GDL, and the power generation continues at the catalyst layer, even under the blocked channel. Thus, water continues

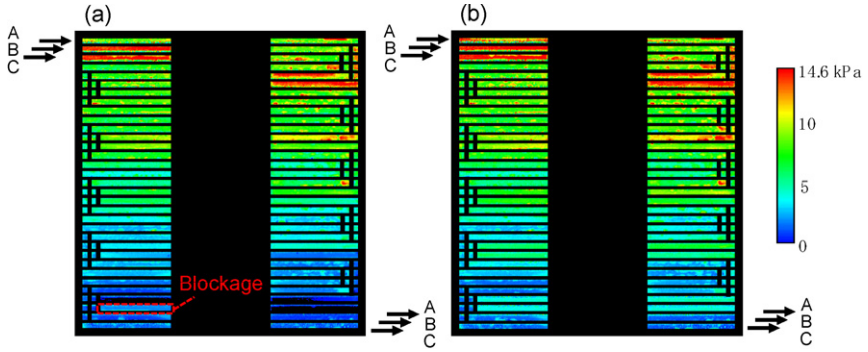

Fig. 7. Oxygen partial pressures visualized in an operating PEFC: with a water blockage in Channel A (a) and after the removal of the water blockage (b).

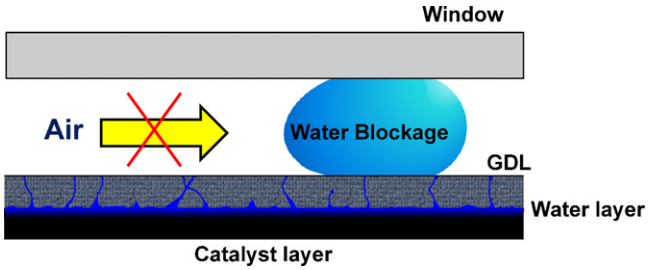

Fig. 9. Schematic drawing of the channel, gas diffusion layer, and catalyst layer with a water blockage.

to be produced at the catalytic layer under the channel blocked by water. The water layer produced at the catalytic layer under the blocked channel might not be easily removed, because of the limitation of gas flow due to the blockage. It is believed that the interface between the catalyst layer and the GDL should be most flooded by the water produced, which could hinder the air access to the catalyst surfaces. In this situation, even though the water droplet in the channel is blown out from the cell, the catalyst layer is still wet, and thus the oxygen consumption is low in the channel, and the oxygen partial pressure remains high. This scenario might have occurred in Fig. 7. In our experiment, it required several minutes for the oxygen partial pressure in the "wet" channel to return to its original value, identical to those in the other two channels. This time period might be necessary for the water in the catalyst layer to be removed, so that adequate power generation in the channel could be recovered. Such a flooded area may expand with operation time and thus may cause significant performance and efficiency losses in the fuel cell (Fig. 9).

4. Conclusions

Oxygen partial pressures and water blockages were visualized simultaneously in a triple-serpentine PEFC, and the relationship between the two was investigated. The oxygen partial pressure in the gas flow channel around the water blockages decreased to nearly 0 kPa. Along the channel from the entrance to the blocking position, however, the oxygen pressure was not 0 kPa, in spite of continuous oxygen consumption, suggesting the transfer of gas through the GDL from the other channels. Thus, even in the blocked channel, electricity can be generated and water be formed with the consumption of oxygen through the GDL. When the water blockage was swept away, the oxygen partial pressure along the channel showed a sudden increase. The higher oxygen pressure along the whole channel compared to that of the normal one can be explained by the lower oxygen consumption because of flooding of the catalyst layer by the accumulation of water, correlating strongly with the cell performance losses. Therefore, the application of the newly developed visualization system to operating fuel cells for the simultaneous observation of oxygen partial pressure and water blockages in the gas-flow channels must be very important for the development of high performance, high durability fuel cells.

Acknowledgements

This work was supported by the New Energy and Industrial Technology Development Organization (NEDO) through the High-Performance Fuel Cells (HiPer-FC) Project. The authors thank Prof. D. Tryk for his help in writing this manuscript.

References

[1] C.Y. Wang, Chem. Rev. 104 (2004) 4727–4766.
[2] Q. Yan, H. Toghiani, H. Causey, J. Power Sources 161 (2006) 492–502.
[3] B. Bae, T. Yoda, K. Miyatake, H. Uchida, M. Watanabe, Angew. Chem. Int. Ed. 49 (2010) 317–320.
[4] U. Pasaogullari, C.Y. Wang, J. Electrochem. Soc. 151 (2004) A399–A406.
[5] H. Li, Y. Tang, Z. Wang, Z. Shi, S. Wu, D. Song, J. Zhang, K. Fatih, J. Zhang, H. Wang, Z. Liu, R. Abouatallah, A. Mazza, J. Power Sources 178 (2008) 103–117.
[6] W. Vielstich, A. Lamm, H.A. Gasteiger (Eds.), Handbook of Fuel Cells: Fundamentals, Technology and Applications, vol. 3, John Wiley & Sons, West Sussex, England, 2003.
[7] K. Tüber, D. Pócza, C. Hebling, J. Power Sources 124 (2003) 403–414.
[8] X. Liu, H. Guo, F. Ye, C.F. Ma, J. Electrochim. Acta 52 (2007) 3607–3614.
[9] D. Spernjak, A.K. Prasad, S.G. Advani, J. Power Sources 170 (2007) 334–344.
[10] M. Yamauchi, K. Sugiura, T. Yamauchi, T. Taniguchi, Y. Itoh, J. Power Sources 193 (2009) 1–8.
[11] R. Satija, D.L. Jacobson, M. Arif, S.A. Werner, J. Power Sources 129 (2004) 238–245.
[12] D. Kramer, J. Zhang, R. Shimoi, E. Lehmann, A. Wokaun, K. Shinohara, G.G. Scherer, Electrochim. Acta 50 (2005) 2603–2614.
[13] M.A. Hickner, N.P. Siegel, K.S. Chen, D.N. McBrayer, D.S. Hussey, D.L. Jacobson, M. Arif, J. Electrochem. Soc. 153 (2006) A902–A908.
[14] Y.-S. Chen, H. Peng, D.S. Hussey, D.L. Jacobson, D.T. Tran, T. Abdel-Baset, M. Biernacki, J. Power Sources 170 (2007) 376–386.
[15] K. Teranishi, S. Tsushima, S. Hirai, J. Electrochem. Soc. 153 (2006) A664–A668.
[16] K.W. Feindel, S.H. Bergens, R.E. Wasylishen, Phys. Chem. Chem. Phys. 9 (2007) 1850–1857.
[17] J. Bedet, G. Maranzana, S. Leclerc, O. Lottin, C. Moyne, D. Stemmelen, P. Mutzenhardt, D. Canet, Int. J. Hydrogen Energy 33 (2008) 3146–3149.
[18] P.K. Sinha, P.P. Mukherjee, C.-Y. Wang, J. Mater. Chem. 17 (2007) 3089–3103.
[19] S.J. Lee, N.-Y. Lim, S. Kim, G.-G. Park, C.-S. Kim, J. Power Sources 185 (2008) 867–870.
[20] T. Mukaide, S. Mogi, J. Yamamoto, A. Morita, S. Koji, K. Takada, K. Uesugi, K. Kajiwara, T. Noma, J. Synchrotron Rad. 15 (2008) 329–334.
[21] A.D. Le, B. Zhou, Electrochim. Acta 54 (2009) 2137–2154.
[22] J. Inukai, K. Miyatake, K. Takada, M. Watanabe, T. Hyakutake, H. Nishide, Y. Nagumo, M. Watanabe, M. Aoki, H. Takano, Angew. Chem. Int. Ed. 47 (2008) 2792–2795.
[23] J. Inukai, K. Miyatake, Y. Ishigami, M. Watanabe, T. Hyakutake, H. Nishide, Y. Nagumo, M. Watanabe, A. Tanaka, Chem. Commun. (2008) 1750–1752.